Murdoch
UNIVERSITY

MURDOCH RESEARCH REPOSITORY

This is the author's final version of the work, as accepted for publication following peer review but without the publisher's layout or pagination. The definitive version is available at
http://dx.doi.org/10.1016/j.electacta.2011.02.100

Yu, A., Zhang, X., Zhang, H., Hannan, D. and Knight, A.R. (2011) Preparation and electrochemical properties of gold nanoparticles containing carbon nanotubes-polyelectrolyte multilayer thin films. Electrochimica Acta, 56 (25). pp. 9015-9019.

http://researchrepository.murdoch.edu.au/5731/

Copyright: © 2011 Elsevier Ltd.

It is posted here for your personal use. No further distribution is permitted.

Accepted Manuscript

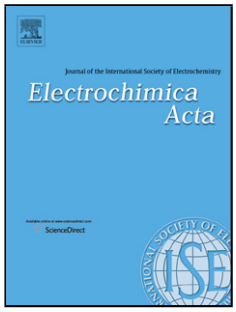

Title: Preparation and Electrochemical Properties of Gold Nanoparticles Containing Carbon Nanotubes-Polyelectrolyte Multilayer Thin Films

Authors: Aimin Yu, Xing Zhang, Haili Zhang, Deyan Han, Allan Knight

PII: S0013-4686(11)00327-6
DOI: doi:10.1016/j.electacta.2011.02.100
Reference: EA 16842

To appear in: *Electrochimica Acta*

Received date: 2-12-2010
Revised date: 22-2-2011
Accepted date: 24-2-2011

Please cite this article as: A. Yu, X. Zhang, H. Zhang, D. Han, A. Knight, Preparation and Electrochemical Properties of Gold Nanoparticles Containing Carbon Nanotubes-Polyelectrolyte Multilayer Thin Films, *Electrochimica Acta* (2008), doi:10.1016/j.electacta.2011.02.100

This is a PDF file of an unedited manuscript that has been accepted for publication. As a service to our customers we are providing this early version of the manuscript. The manuscript will undergo copyediting, typesetting, and review of the resulting proof before it is published in its final form. Please note that during the production process errors may be discovered which could affect the content, and all legal disclaimers that apply to the journal pertain.

*Revised Manuscript (including Abstract)
Click here to view linked References
ACCEPTED MANUSCRIPT

Preparation and Electrochemical Properties of Gold Nanoparticles Containing Carbon Nanotubes-Polyelectrolyte Multilayer Thin Films

Aimin Yu[a,b,*], Xing Zhang[a,c], Haili Zhang[a], Deyan Han[a] and Allan Knight[c]

[a]*College of Chemical and Environmental Engineering, Hubei Normal University, 435002, China*

[b]*Faculty of Life and Social Sciences, Swinburne University of Technology, Hawthorn VIC 3122, Australia*

[c]*School of Chemical and Mathematic Sciences, Murdoch University, Murdoch WA 6150, Australia*

[*] Corresponding author. E-mail: aiminyu@swin.edu.au.

Tel: +61-3-9214 8161; Fax: +61-3-9819 0574

Accepted Manuscript

ACCEPTED MANUSCRIPT

ABSTRACT

Multi-walled carbon nanotubes (MWCNT)/polyelectrolyte (PE) hybrid thin films were fabricated by alternatively depositing negatively charged MWCNT and positively charged (diallyldimethylammonium chloride) (PDDA) via layer-by-layer (LbL) assembly technique. The stepwise growth of the multilayer films of MWCNT and PDDA was characterized by UV-vis spectroscopy. Scanning electron microscopy (SEM) images indicated that the MWCNT were uniformly embedded in the film to form a network and the coverage density of MWCNT increased with layer number. Au nanoparticles (NPs) could be further adsorbed onto the film to form Au NPs/MWCNT composite films. The electron transfer behaviour of multilayer films with different compositions were studied by cyclic voltammetry using $[Fe(CN)_6]^{3-/4-}$ as an electrochemical probe. The results indicated that the incorporation of MWCNT and Au NPs not only greatly improved the electronic conductivity of pure polyelectrolyte films, but also provided excellent electrocatalytic activity towards the oxidation of nitric oxide (NO).

Keywords: Multilayer thin films, Carbon nanotubes, Gold nanoparticles, Electrocatalysis, Layer-by-layer

Accepted Manuscript

ACCEPTED MANUSCRIPT

1. Introduction

The development of functional nanostructured materials is currently one of the most active research fields. Since its discovery in 1991, carbon nanotubes (CNTs) with unique properties of high electrical conductivity, superior chemical and mechanical stability, and large surface area [1,2] has been one of the most promising materials for applications in many scientific and technological fields such as actuation [3,4], catalytic membranes [5,6], polymer composites [7,8], electrochemical energy conversion and storage devices [9-12] and biological systems [13,14]. However, due to the strong van der Waals interactions between tubes, CNTs tend to precipitate into ropes or bundles in the solution resulting in a phase separation. In order to be used in the solution processes and take advantage of their unique properties, it is necessary to tailor the chemical nature of the nanotube's wall to solubilize and separate discrete CNT molecules from the tight bundles. For this purpose, several approaches have been developed for the surface modification of CNTs including chemical functionalization using strong acids treatment [15-17], covalent attachment of functional groups to the walls of the nanotubes [18-20], and wrapping nanotubes with surfactants or polymers [21-25]. Among them, the non-covalent polymer wrapping method has the advantage of being a mild procedure which avoids the usage of strong acids and has less destructive to the intrinsic properties of CNT [23].

So far, CNT-based films can be fabricated by various techniques such as vacuum filtration [26], drop-casting [27], spin-coating [28], airbrushing [29], Langmuir-Blodgett (LB) deposition [30] and electrophoretic method [31]. However, most of these techniques lack the ability either to control the architecture or tailor the properties and functionality of the films. Recently, layer-by-layer (LbL) self-assembly technique, which introduced by Decher and Hong in 1991 [32], has emerged as a simple, versatile and promising approach to fabricate

Accepted Manuscript

ACCEPTED MANUSCRIPT

functional molecular assemblies with well-defined architectures and with nanoscale-level control over the film thickness [33,34]. The basis of this method is the stepwise electrostatic assembly of oppositely charged species. The pioneer work of preparation of CNT multilayer films using LbL was reported by Kotov in 2002. In this work, single-walled carbon nanotube (SWCNT) was treated with 65% HNO_3 to oxidize the surface carbon to obtain a negative charge. Free-standing SWCNT/polymer membranes with a tensile strength approaching that of hard ceramics were prepared by LbL assembly with positively charged polyelectrolyte [35]. Since then, there have been increasing reports on preparing CNT multilayer films with various components and functionalities [9,17,36-39]. For example, Lee et al. reported the preparation of multilayer films comprising multi-walled carbon nanotubes (MWCNT) and TiO_2 nanoparticles in a non-polar solvent and the incorporated MWCNT exhibited significant enhancement to the photocatalytic activity of TiO_2 [37]. MWCNT-poly(allylamine hydrochloride) (PAH) films were prepared by LbL assembly and used as reverse osmosis (RO) membranes for desalination. MWCNT was shown to be effective in enhancing the mechanical strength of the membrane and reducing the salt rejection [38]. A recent interesting work of Hammond's group demonstrated that all CNT films could be prepared by LbL assembly of two oppositely charged MWCNTs and the resulting films exhibited higher electronic conductivity in comparison with polymer/CNT composites [17].

In the present study, we report the dispersing MWCNT using a negatively charged linear polyelectrolyte poly (sodium 4-styrene-sulfonate) (PSS). The resulting PSS wrapped CNT are then used as building blocks to form multilayer films with positively charged polyelectrolyte PDDA using the LbL approach. The LbL technique also affords the preparation of gold nanoparticles (Au NPs)-MWCNT composite film by further immobilizing Au NPs onto the MWCNT film. Au NPs possess unique optical, electronic and catalytic properties, and therefore have been another promising building block for the fabrication of functional

Accepted Manuscript

ACCEPTED MANUSCRIPT

materials [40-46]. UV-Vis spectroscopy is employed to characterize the stepwise growth of the multilayer film and the adsorption behavior of Au NPs onto the preformed MWCNT multilayer film. The effect of CNT and Au NPs on the conductivity and electron transfer behaviour of the polyelectrolyte films is then studied using $[Fe(CN)_6]^{3-/4-}$ as an electrochemical probe. In addition, we also explore the electrocatalytic behavior of the MWCNT/Au NPs composite film towards the oxidation of a small molecule of nitric oxide which is an important messenger molecule involved in many physiological and pathological processes within the mammalian bodies [47,48].

2. Experimental

2.1. Chemicals and materials

Poly (diallyldimethylammonium chloride) (PDDA, *M*w = 100 000–200 000, 20 wt. % in water), poly (sodium 4-styrene-sulfonate) (PSS, *Mw* = 70 000), poly (ethylenimine) (PEI, *Mw* = 25 000, water-free), hydrogen tetrachloroaurate trihydrate ($HAuCl_4 \cdot 3H_2O$) were purchased from Sigma-Aldrich. Multi-walled carbon nanotubes (purity ≥ 95%, diameters 10-30 nm, length 1-2 μm) were purchased from Shenzhen Nanotech Port Co. Ltd. (China). All other chemicals used were analytical grade reagents and used without further purification. ITO coated glasses (R_{est} = 1 0 ± 2 Ω) were purchased from Delta Technologies (USA). 4-dimethylaminopyridine-stabilized Au NPs (~ 5 nm) were synthesized according to the previous literature [49]. PE (PEI, PSS and PDDA) solutions of 1 mg mL^{-1} in water containing 0.5 M NaCl were used for depositing individual PE layer. Phosphate buffer (PB) solutions of different pH were prepared by mixing 0.1 M H_3PO_4, KH_2PO_4 and K_2HPO_4. The

Accepted Manuscript

ACCEPTED MANUSCRIPT

water used in all experiments was prepared in a Milli-Q system and had a resistivity higher than 18.2 MΩ cm.

2.2. Preparation of MWCNT dispersion

5 mg as-received MWCNT were added into a 10 mL aqueous solution of 10 mg/mL PSS. After sonication for 4 h or until a homogeneous black suspension was achieved, excess PSS was removed by two repeated centrifugation (20000 rpm, 40 min)/water wash/redispersion cycles. The final PSS-wrapped MWCNT (denoted as MWCNT throughout this work) water dispersion had a concentration of about 0.5 mg mL^{-1}.

2.3. Construction of Au NPs containing PE/MWCNT multilayer thin films

Multilayer thin films were deposited either on quarts slides or ITO electrodes which were cleaned by using the RCA protocol (placing in a 5:1:1 (v/v/v) $H_2O/H_2O_2/NH_3$ bath at 70 ^oC for 30 min), followed by extensive rinsing with Milli-Q water. The cleaned substrates were first modified with a "precursor" film of PEI/PSS, which was formed by the alternate deposition of PEI and PSS from the corresponding PE solutions for 15 min, followed by rinsing in pure water (three times each for 1 min) and drying with a gentle stream of N_2. Alternative layers of PDDA and MWCNT were then deposited on the substrate using the same procedure until the desired number of layers was deposited. Au NPs could be adsorbed onto the film (with MWCNT as the outermost layer) by immersing the film coated substrate into the gold nanoparticles suspension for 1 h. The final film was denoted as $(PDDA/MWCNTS)_n$/Au NPs (n = 1, 2, 3...).

Accepted Manuscript

ACCEPTED MANUSCRIPT

2.4. Characterization

UV-vis spectra of the assembled films on quartz slides were recorded on a Hewlett-Packard 8452 spectrophotometer (Agilent, Palo Alto, CA). Top-view Scanning Electron Microscopy (SEM) images of thin films were obtained with a XL 30 FEG (Philips) instrument operated at an acceleration voltage of 10 kV. Thin gold film was coated before measurements.

2.5. Electrochemical measurements

The electrochemical experiments were carried out in a conventional three-electrode electrochemical cell comprising a gold wire as the auxiliary electrode, a saturated calomel electrode (SCE) as reference electrode, against which all potentials are quoted, and thin films coated ITO glasses as working electrodes. The electrodes were connected to a potentiostat (eDAQ, Australia). All measurements were performed at room temperature.

3. Results and discussion

3.1. MWCNT/PDDA multilayer film assembly

Uniform and stable MWCNT water dispersion was prepared using a polyelectrolyte wrapping method. Fig. 1b shows the UV-vis absorption spectroscopy of the as prepared PSS modified MWCNT water dispersion. As pure PSS has absorption at 228 and 262 nm (Fig. 1a), the peak centred at 262 nm in Fig. 1b is attributed to the absorption of PSS which gives evidence of the attachment of PSS on MWCNT. The driving force for PSS adsorbing onto

Accepted Manuscript

ACCEPTED MANUSCRIPT

pristine CNT is mainly due to the π-π stacking and van der Waals interactions between the surface of CNT and the aromatic ring of PSS [23].

The adsorption of PSS brings the negative charge to MWCNT which enables the construction of multilayer films with positively charged polyelectrolyte PDDA via LbL self-assembly technique. UV-vis absorption spectroscopy is used to monitor the MWCNT/PDDA multilayer film growth on a quartz substrate. As shown in Fig. 2, the film exhibits two absorption peaks at 230 and 268 nm which are due to the absorption of PDDA and PSS on CNT. The total absorbance increases gradually with increasing layer number indicating a regularly stepwise growth of the film which confirms the successful formation of a MWCNT/PDDA multilayer film. Fig. 2 inset shows the absorbance at 270 nm as a function of the bilayer numbers. The result indicates that the multilayer film exhibits a nonlinear growth, i.e. the material adsorbed on the surface increases more than linearly with the number of deposited layers. The nonlinear growth of the film has been observed in multilayer films comprising a weak polyelectrolyte and explained by a "diffusion in and diffusion out" mechanism [50-52]. However, in this case, we believe the nonlinear growth trend, though not exponential, is more likely caused by the gradual increase of the effective surface area of the film due to MWCNT deposition. The embedment of MWCNT might slightly increase the surface area of film resulting in adsorbing more polyelectrolyte and MWCNT in the next deposition cycles.

The surface morphology of PDDA/MWCNT hybrid films was then investigated by SEM. Fig. 3a and b presents the top-view SEM images of PDDA/MWCNT films with different bilayer numbers. It is clearly seen that MWCNT are embedded in the film but in a random state to form a network. The diameters of MWCNT are in the range of 20-30 nm which are close to the size of individual MWCNT stated by the manufacture. The appearance of individual MWCNT indicates that PSS is an efficient wrapping agent at breaking up

Accepted Manuscript

ACCEPTED MANUSCRIPT

nanotube bundles and also there is no obvious aggregation occurring during film assembly. Further comparing the morphology of films deposited with different layer of CNT, a much higher CNT coverage is observed for film with 6 layers of CNT deposition (Fig. 3b). The SEM results further confirm that the no-covalent interaction between MWCNT and the oppositely charged polyelectrolyte could allow the formation of a CNT/polyelectrolyte hybrid film and the MWCNT surface coverage could be controlled by the deposition layer number.

3.2. Au NPs adsorption onto PDDA/MWCNT multilayer film

Au NPs could be assembled onto the PDDA/MWCNT multilayer film by simply exposing the film slide in Au NPs colloidal solution. The adsorption of Au NPs onto the film was confirmed by UV-vis spectroscopy. Before Au NPs adsorption, quartz slide coated with $(PDDA/MWCNT)_2$ film shows no absorption in the wavelength range between 400 and 800 nm (Fig. 4a). In contrast, a clear absorption band centred at 580 nm appears after Au NPs adsorption (curve b) which is attributed to the plasmon absorption of gold nanoparticles. The relatively sharp plasmon peak indicates that the adsorbed Au nanoparticles do not undergo obvious aggregation to form larger clusters after adsorption. However, there is a 58 nm red-shift in surface plasmon band compared with that of the colloidal Au NPs solution (522 nm), which can be explained as a result of reduced nanoparticle - nanoparticle distance (i.e., more dense packing) in the film and also due to the change of refractive index as a result of the surrounding PE matrix [53]. Further experiments were carried out on monitoring the adsorption of Au NPs on PDDA/MWCNT films with different layer number (n = 2, 4, 6). The resulting absorption spectra reveal that the gold nanoparticle plasmon absorbance change due to the adsorption of Au NPs is about the same for these three films (compare curves c and d with b). The results indicate that the original film thickness does not significantly affect the

ACCEPTED MANUSCRIPT

adsorbing amount of Au NPs which suggests that instead of being able to infiltrate into the multilayer film, Au NPs are more likely only adsorbing at the outmost layer of the film.

3.3. Electrochemical behaviour of the multilayer films

$K_3Fe[CN]_6$ is a substance that undergoes reversible electrochemical reaction on various electrodes, which is widely used as an electrochemical probe to investigate the electrochemical behaviour of films with different composition [54,55]. Fig. 5a, shows the cyclic voltammograms (CVs) of bare ITO electrode in pH 7.0 phosphate buffer (PB) solution containing 10 mM $K_3Fe[CN]_6$. It can be seen that in the potential region from -0.2 to 0.7 V, $K_3Fe[CN]_6$ exhibits a pair of well-defined redox peaks at 0.42 V and 0.07 V. However, there is no visible current response for $K_3Fe[CN]_6$ after the same electrode coated with eight layers of PEs (PEI/PSS/$(PDDA/PSS)_3$), (curve b). This is due to the non-conductive nature of the polyelectrolytes resulting in sluggish electron-transfer kinetics through the PE film. We then replace PSS with MWCNT as building blocks for film construction and a pair of reversible peaks of $K_3Fe[CN]_6$ is observed at PEI/PSS/$(PDDA/MWCNT)_3$ modified electrode (curve c). Compared with CV at bare ITO electrode (curve a), a higher current response and a slight smaller peak separation (ΔE_p, the potential difference between the oxidation peak potential and the reduction peak potential, which is inversely proportional to the electron transfer rate [56]) is observed. The results indicate that the incorporation of MWCNT could significantly improve the electron transfer behaviour of a PE film due to its excellent electronic conductivity. By further depositing gold nanoparticles on the PE/MWCNT electrode, a higher current response and smaller peak separation (ΔE_p= 420 mV) could be achieved (curve d). These results reveal that Au NPs have the similar role as MWCNT to improve the electron

Accepted Manuscript

ACCEPTED MANUSCRIPT

transfer between $K_3Fe[CN]_6$ and the electrode. The presence of gold nanoparticles could also increase the effective electrode surface area resulting in a higher current response.

Further investigation was made into the electrocatalytic activity of Au NPs/MWCNT thin film to nitric oxide. Free NO can be generated in an acid solution using sodium nitrite ($NaNO_2$) as a precursor [57,58]. Fig. 6 presents CVs obtained at electrodes coated with different films in pH 2.0 PB buffer containing 0.6 mM $NaNO_2$. NO shows no current response at the bare ITO electrode (curve a). After the electrode was modified with 3 layers of MWCNT, an oxidation peak appears at ~0.92 V (curve b), which indicates that MWCNT can catalyze the oxidation of NO. Curve c shows the CV of PEI/PSS/$(PDDA/MWCNT)_3$/Au NPs modified electrode in the same NO solution. A similar oxidation peak located at 0.88 V is observed but with a much higher current response. Our previous research had shown that Au NPs are catalytic towards the oxidation of NO [40]. The results here indicate that a film combined with Au NPs and MWCNT has a greater effect on electrocatalytic activity towards the oxidation of NO, resulting in a much higher current response. The larger background current observed at Au NPs modified film is another evidence of the increase in effective electrode surface area due to the deposition of Au NPs (see above).

Successive addition of a stock nitrite solution into the bulk solution was made to generate a series of concentrations of NO. Fig. 7 shows the CVs of a PEI/PSS/$(PDDA/MWCNT)_3$/Au NPs coated electrode at different $NaNO_2$ concentrations. The anodic peak current (i_{pa}) increases linearly with increasing $NaNO_2$ concentration (Fig. 7, inset) indicates the applicability of using MWCNT/Au NPs composite electrode for the measurement of NO.

4. Conclusions

Accepted Manuscript

ACCEPTED MANUSCRIPT

In this work, we have shown that well dispersed MWCNT solution could be prepared via a simple PSS wrapping method and the resulting MWCNT could be used as building blocks to form multilayer films with oppositely charged polyelectrolyte PDDA via electrostatic LbL self-assembly technique on quartz slides and ITO glasses. UV-vis absorption spectra confirmed the stepwise regular growth of the multilayer film and SEM images indicated a random distribution of MWCNT in the film. Au NPs could be further adsorbed onto the PE/MWCNT film but without being able to infiltrate into the multilayer. Electrochemical experiments revealed that Au NPs and MWCNT could both greatly improve the conductivity and electron transfer of PE films. Additionally, the electrocatalytic properties of MWCNT could be exploited to the electrochemical detection of NO, while the sensitivity of the film could be further improved by the presence of gold nanoparticles.

Acknowledgments

The authors gratefully acknowledge the support from the National Natural Science Foundation of China (21075030) and Australian Research Council under its Discovery Project Scheme (DP0776086).

References

[1] T.W. Odom, J.L. Huang, P. Kim, C.M. Lieber, Nature 391 (1998) 62.

[2] R.H. Baughman, A. Zakhilov, W. . de Heer, Science 297 (2002) 787.

[3] R.H. Baughman, C.X. Cui, A.A. Zakhidov, Z. Iqbal, J.N. Barisci, G. . Spinks, G.G. Wallace, A. Mazzoldi, D. de Rossi, A.G. Rinzler, O. Jaschinski, S. Roth, M. Kertesz, Science 284 (1999) 1340.

Accepted Manuscript

ACCEPTED MANUSCRIPT

[4] B.J. Landi, R.P. Raffaelle, M.J. Heben, J.L. Alleman, W. van Derveer, T. Gennett, Nano Lett. 2 (2002) 1329.

[5] J.K. Holt, H.G. Park, Y.M. Wang, M. Stadermann, A.B. Artyukhin, C.P. Grigoropoulos, A. Noy, O. Bakajin, Science 312 (2006) 1034.

[6] R. Smajda, A. Kukovecz, Z. Konya, I. Kiricsi, Carbon 45 (2007) 1176.

[7] L.S. Schadler, S.C. Giannaris, P.M. Ajayan, Appl. Phys. Lett. 73 (1998) 3842.

[8] D. Qian, E.C. Dickey, R. Andrews, T. Rantell, Appl. Phys. Lett. 76 (2000) 2868.

[9] M. Michel, A. Taylor, R. Sekol, P. Podsiadlo, P. Ho, N.A. Kotov, L. Thompson, Adv. Mater. 19 (2007) 3859.

[10] R.S. Morris, B.G. Dixon, T. Gennett, R. Raffaelle, M.J. Heben, J. Power Sources 138 (2004) 277.

[11] D.N. Futaba, K. Hata, T. Yamada, T. Hiraoka, Y. Hayamizu, Y. Kakudate, O. Tanaike, H. Hatori, M. Yumura, S. Iijima, Nat. Mater. 5 (2006) 987.

[12] B.J. Yoon, S.H. Jeong, K.H. Lee, H.S. Kim, C.G. Park, J.H. Han, Chem. Phys. Lett. 388 (2004) 170.

[13] R.J. Chen, Y. Zhang, D. Wang, H. Dai, J. Am. Chem. Soc. 123 (2001) 3838.

[14] N.W.S. Kam, E. Jan, N.A. Kotov, Nano Lett. 9 (2009) 273.

[15] J. Liu, A. G. Rinzler, H.J. Dai, J.H. Hafner, R.K. Bradley, P.J. Boul, A. Lu, T. Iverson, K. Shelimov, C.B. Huffman, F. Rodriguez-Macias, Y.S. Shon, T.R. Lee, D.T. Colbert, R.E. Smalley, Science 280 (1998) 1253.

[16] K. Esumi, M. Ishigami, A. Nakajima, K. Sawada, H. Honda, Carbon 34 (1996) 279.

[17] S.W. Lee, B.S. Kim, S. Chen, S.H. Yang, P.T. Hammond, J. Am. Chem. Soc. 131 (2009) 671.

[18] D. Tasis, N. Tagmatarchis, V. Georgakilas, M. Prato, Chem. Eur. J. 9 (2003) 4000.

[19] S.E. Kooi, U. Schlecht, M. Burghard, K. Kern, Angew Chem. Int. Ed. 41 (2002) 1353.

[20] J.L. Bahr, E.T. Mickelson, M.J. Bronikowski, R.E. Smalley, J.M. Tour, Chem. Commun. (2001) 193.

[21] M.J. O'Connell, P. Boul, L.M. Ericson, C. Huffman, Y.H. Wang, E. Haroz, C. Kuper, J. Tour, K.D. Ausman, R.E. Smalley, Chem. Phys. Lett. 342 (2001) 265.

Accepted Manuscript

ACCEPTED MANUSCRIPT

[22] A. Satake, Y. Miyajima, Y. Kobuke, Chem. Mater. 17 (2005) 716.

[23] P. Liu, Eur. Polym. J. 41 (2005) 2693.

[24] J.Y. Hwang, A. Nish, J. Doig, S. Douven, C.W. Chen, L.C. Chen, R.J. Nicholas, J. Am. Chem. Soc. 130 (2008) 3543.

[25] F. Rivadulla, C. Mateo-Mateo, M.A. Correa-Duarte, J. Am. Chem. Soc. 132 (2010) 3751.

[26] A.A. Green, M.C. Hersam, Nano Lett. 8 (2008) 1417.

[27] T.V. Sreekumar, T. Liu, S. Kumar, L.M. Ericson, R.H. Hauge, R.E. Smalley, Chem. Mater. 15 (2003) 175.

[28] M.A. Meitl, Y.X. Zhou, A. Gaur, S. Jeon, M.L. Usrey, M.S. Strano, J.A. Rogers, Nano Lett. 4 (2004) 1643.

[29] G. Gruner, J. Mater. Chem. 16 (2006) 3533.

[30] X. Yu, R. Rajamani, K.A. Stelson, T. Cui, Surf. Coat. Technol. 202 (2008) 2002.

[31] A.R. Boccaccini, J. Cho, J.A. Roether, B.J.C. Thomas, E.J. Minay, M.S.P. Shaffer, Carbon 44 (2006) 3149.

[32] G. Decher, J.D. Hong, Ber. Bunsenges. Phys. Chem. 95 (1991) 1430.

[33] For a review, see: G. Decher, Science 277 (1997) 1232.

[34] For a recent review, see: T. Boudou, T. Crouzier, K.F. Ren, G. Blin, C. Picart, Adv. Mater. 22 (2010) 441.

[35] A.A. Mamedov, N.A. Kotov, M. Prato, D.M. Guldi, J.P. Wicksted, A. Hirsch, Nat. Mater. 1 (2002) 190.

[36] A.D. Taylor, M. Michel, R.C. Sekol, J.M. Kizuka, N.A. Kotov, L.T. Thompson, Adv. Funct. Mater. 18 (2008) 3354.

[37] K.E. Tettey, M.Q. Yee, D. Lee, ACS Appl. Mater. Interfaces 2 (2010) 2646.

[38] J. Park, W. Choi, J. Cho, B.H. Chun, S. . Kim, K.B. Lee, J. Bang, Desalination and Water Treatment 15 (2010) 76.

[39] B.S. Kim, S.W. Lee, H. Yoon, M.S. Strano, Y. Shao-Horn, P.T. Hammond, Chem. Mater. 22 (2010) 4791.

[40] A.M. Yu, Z. Liang, J. Cho, F. Caruso, Nano Lett. 3 (2003) 1203.

Accepted Manuscript

ACCEPTED MANUSCRIPT

[41] F.N. Crespilho, V. Zucolotto, C.M.A. Brett, O.N. Oliveira, F.C. Nart, J. Phys. Chem. B 110 (2006) 17478.

[42] H.Y. Gu, Z. Chen, R.X. Sa, S.S. Yuana, H.Y. Chen, Y.T. Ding, A.M. Yu, Biomaterials 25 (2004) 3445.

[43] N. Alexeyeva, K. Tammeveski, Anal. Chim. Acta 618 (2008) 140.

[44] S. Srivastava, N. A. Kotov, Acc. Chem. Res. 41 (2008) 1831.

[45] J. Kim, S.W. Lee, P.T. Hammond, Y. Shao-Horn Chem. Mater. 21 (2009) 2993.

[46] M. Hojeij, B. Su, S.X. Tan, G. Meriguet, H.H. Girault, ACS Nano 2 (2008) 984.

[47] L.J. Ignarro, G.M. Bugga, K.S. Wood, R.E. Byrns, G. Chaudhuri, Proc. Natl. Acad. Sci. USA 84 (1987) 9265.

[48] D.E. Koshland, Science 258 (1992) 1861.

[49] D.I. Gittins, F. Caruso, Angew. Chem. Int. Ed. 40 (2001) 3001.

[50] P. Lavalle, V. Vivet, N. Jessel, G. Decher, J.C. Voegel, P.J. Mesini, P. Schaaf, Macromolecules 37 (2004) 1159.

[51] P. Kujawa, P. Moraille, J. Sanchez, A. Badia, F.M. Winnik, J. Am. Chem. Soc. 127 (2005) 9224.

[52] A.M. Yu, I.R. Gentle, G.Q. Lu, J. Colloid Interface Sci. 333 (2009) 341.

[53] J. Schmitt, P. Mächtle, D. Eck, H. Möhwald, C.A. Helm, Langmuir 15 (1999) 3256.

[54] J.J. Harris, M.L. Bruening, Langmuir 16 (2000) 2006.

[55] V. Pardo-Yissar, E. Katz, O. Lioubashevski, I. Willner, Langmuir 17 (2001) 1110.

[56] A.J. Bard, C.R. Faulkner, Electrochemical Methods: Fundamentals and Applications, 2nd ed.; John Wiley & Sons Inc.: New York, 2000.

[57] G. Stedman, Adv. Inorg. Chem. Radiochem. 22 (1979) 113.

[58] F.A. Cotton, G. Wilkinson, Advanced Inorganic Chemistry, 5th ed.; Wiley: New York, 1988; p 327.

Accepted Manuscript

ACCEPTED MANUSCRIPT

Fig. Captions

Fig. 1. UV-vis absorption spectra of 0.5 mg.mL^{-1} PSS aqueous solution (a) and PSS modified MWCNT water dispersion (b).

Fig. 2. UV-vis absorption spectra of PEI/PSS/(PDDA/MWCNT)$_n$ (n = 2~12) multilayer film on quartz slide. The inset shows the absorbance maximum at 270 nm as the function of the number of bilayers.

Fig. 3. SEM images of [PEI/PSS/(PDDA/MWCNT)$_3$] (a) and [PEI/PSS/(PDDA/MWCNT)$_6$] (b) thin films deposited on quartz slides.

Fig. 4. UV-vis absorption spectra of thin films of [PEI/PSS/(PDDA/MWCNT)$_2$] (a), [PEI/PSS/(PDDA/MWCNT)$_2$/Au NPs] (b), [PEI/PSS/(PDDA/MWCNT)$_4$/Au NPs] (c) and [PEI/PSS/(PDDA/MWCNT)$_6$/Au NPs] (d).

Fig. 5. Cyclic voltammograms of 10 mM $K_3Fe[CN]_6$ in pH 7.0 PB at a bare ITO electrode (a), and ITO electrodes modified with [PEI/PSS/(PDDA/PSS)$_3$] (b), [PEI/PSS(PDDA/MWCNT)$_3$] (c), and [PEI/PSS/(PDDA/MWCNT)$_3$/Au NPs] (d). Scan rate = 50 mV/s.

Fig. 6. Cyclic voltammograms obtained in a pH 2.0 0.6 mM $NaNO_2$ solution using a bare ITO electrode (a), and ITO electrodes modified with [PEI/PSS/(PDDA/MWCNT)$_3$] (b), [PEI/PSS/(PDDA/MWCNT)$_3$/Au NPs] (c). Scan rate = 50 mV/s.

Fig. 7. Cyclic voltammograms of an ITO electrode modified with PEI/PSS/(PDDA/ MWCNT)$_3$ /Au NPs in pH 2.0 PB buffer containing (a) 0, (b) 0.1, (c) 0.2, (d) 0.3, (e) 0.4, (f) 0.5 and (g) 0.6 mM $NaNO_2$. Scan rate = 50 mV/s.

Accepted Manuscript

ACCEPTED MANUSCRIPT

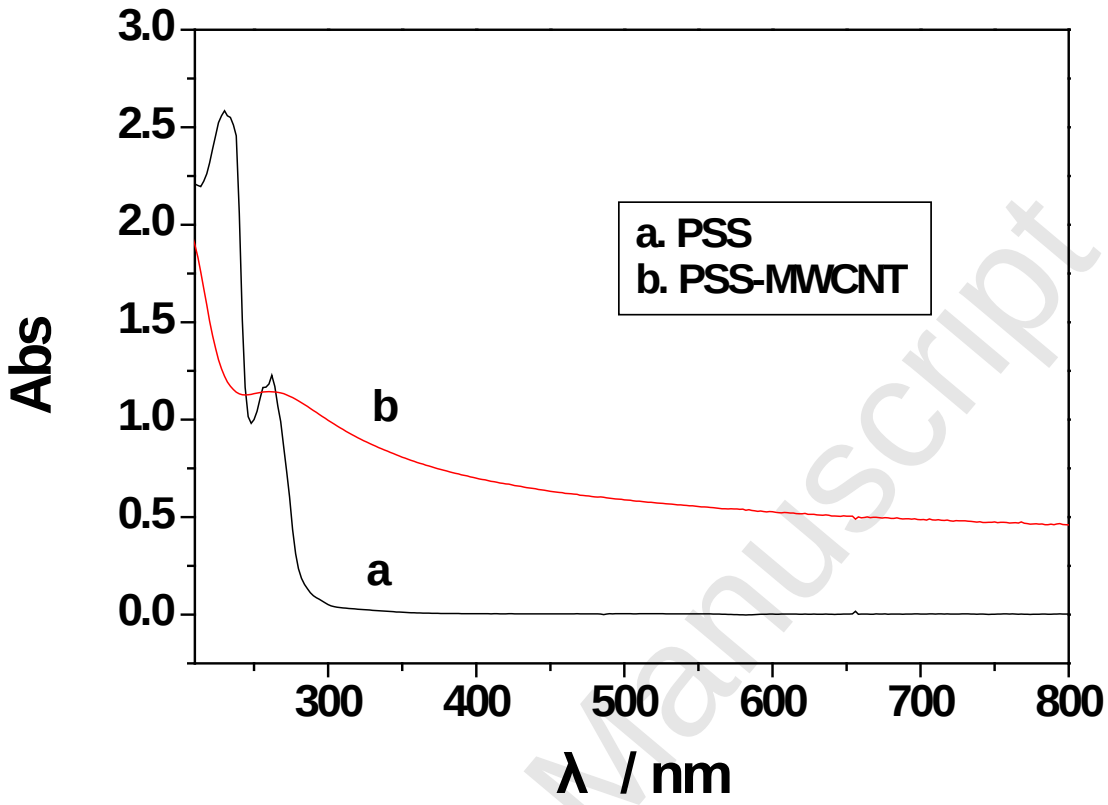

Fig. 1. UV-vis absorption spectra of 0.5 mg.mL^{-1} PSS aqueous solution (a) and PSS modified MWCNT water dispersion (b)

Accepted Manuscript

ACCEPTED MANUSCRIPT

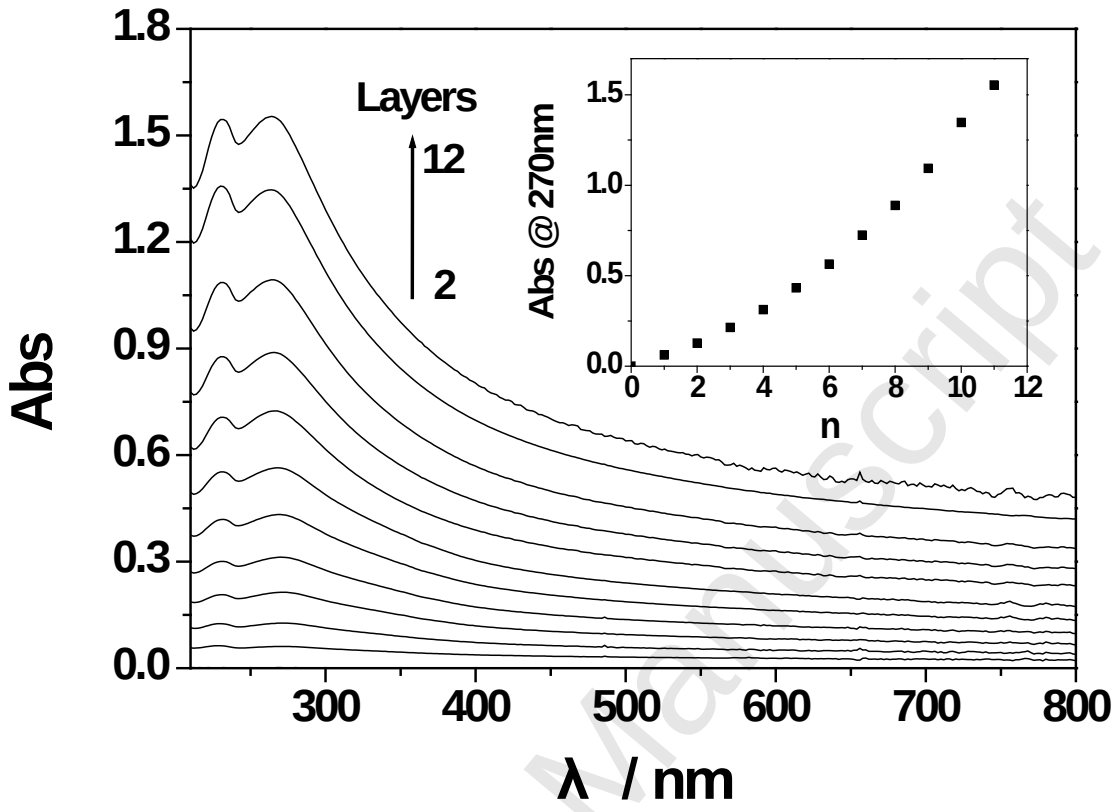

Fig. 2. UV-vis absorption spectra of PEI/PSS/(PDDA/MWCNT)$_n$ (n = 2~12) multilayer films on quartz slide. The inset shows the absorbance maximum at 270 nm as the function of the number of bilayers.

Accepted Manuscript

ACCEPTED MANUSCRIPT

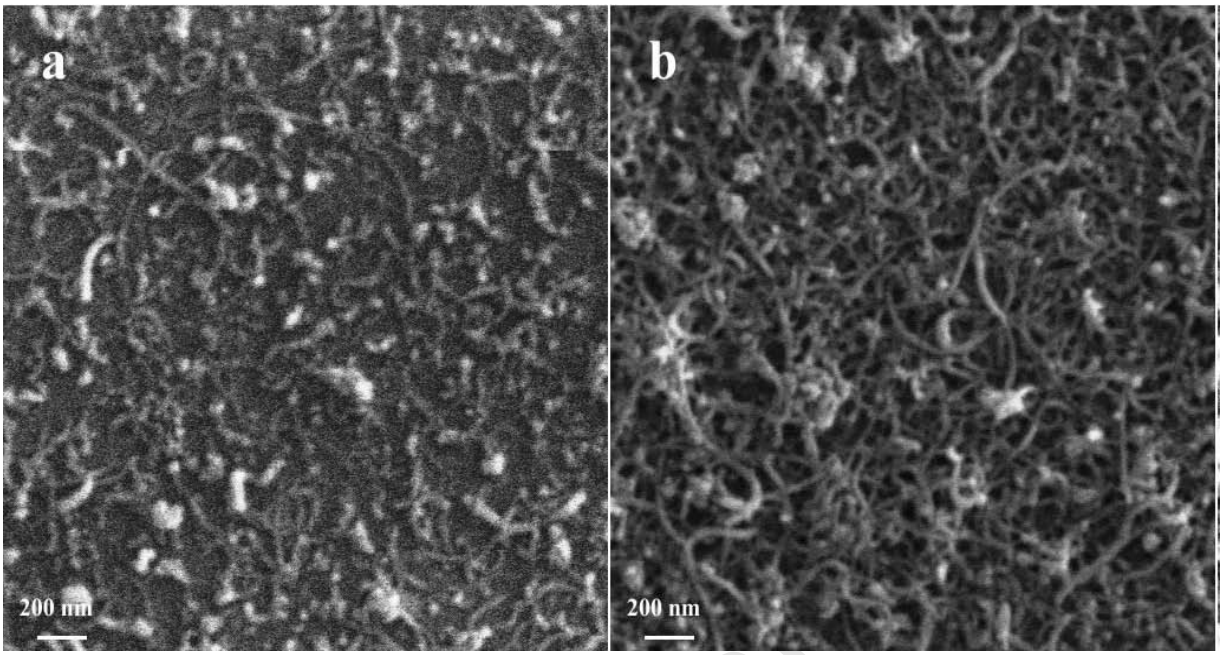

Fig. 3. SEM top-view images of [PEI/PSS/(PDDA/MWCNT)$_3$] (a) and [PEI/PSS/(PDDA/MWCNT)$_6$] (b) thin films deposited on quartz slides.

Accepted Manuscript

ACCEPTED MANUSCRIPT

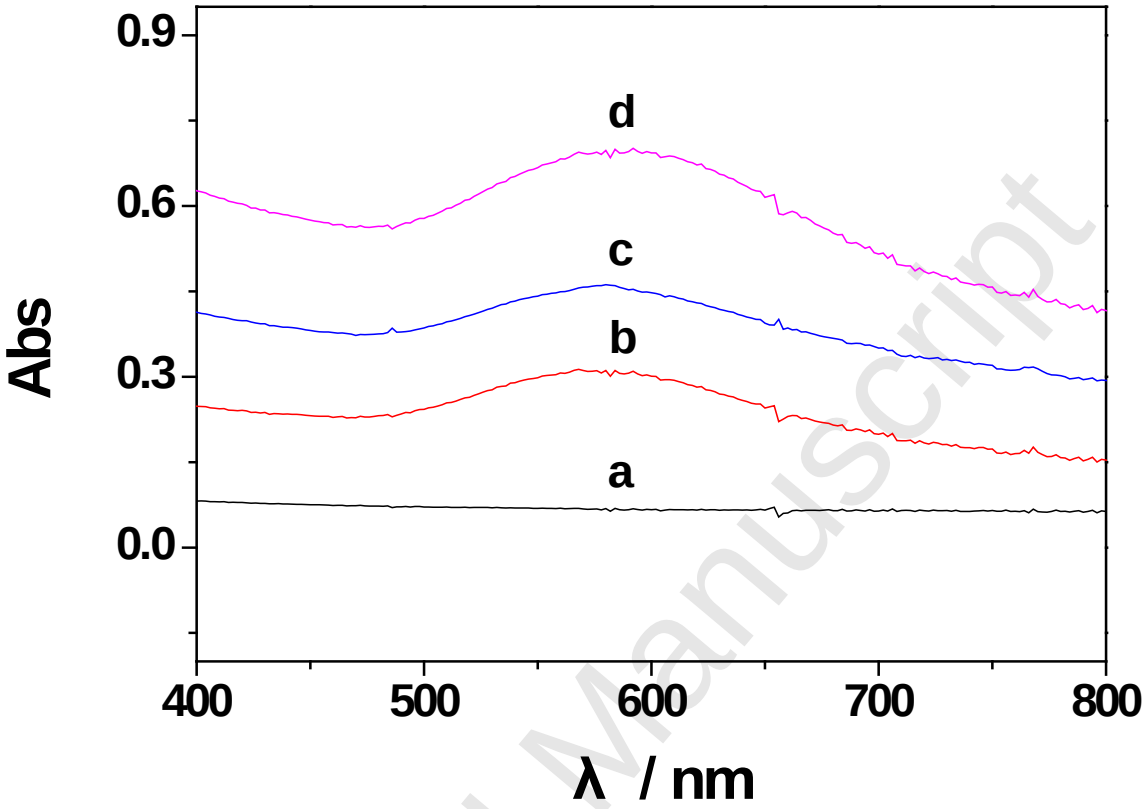

Fig. 4. Absorption spectra of thin films of [PEI/PSS/(PDDA/MWCNT)$_2$] (a), [PEI/PSS/(PDDA/MWCNT)$_2$/Au NPs] (b), [PEI/PSS/(PDDA/MWCNT)$_4$/Au NPs] (c) and [PEI/PSS/(PDDA/MWCNT)$_6$/Au NPs] (d).

Accepted Manuscript

ACCEPTED MANUSCRIPT

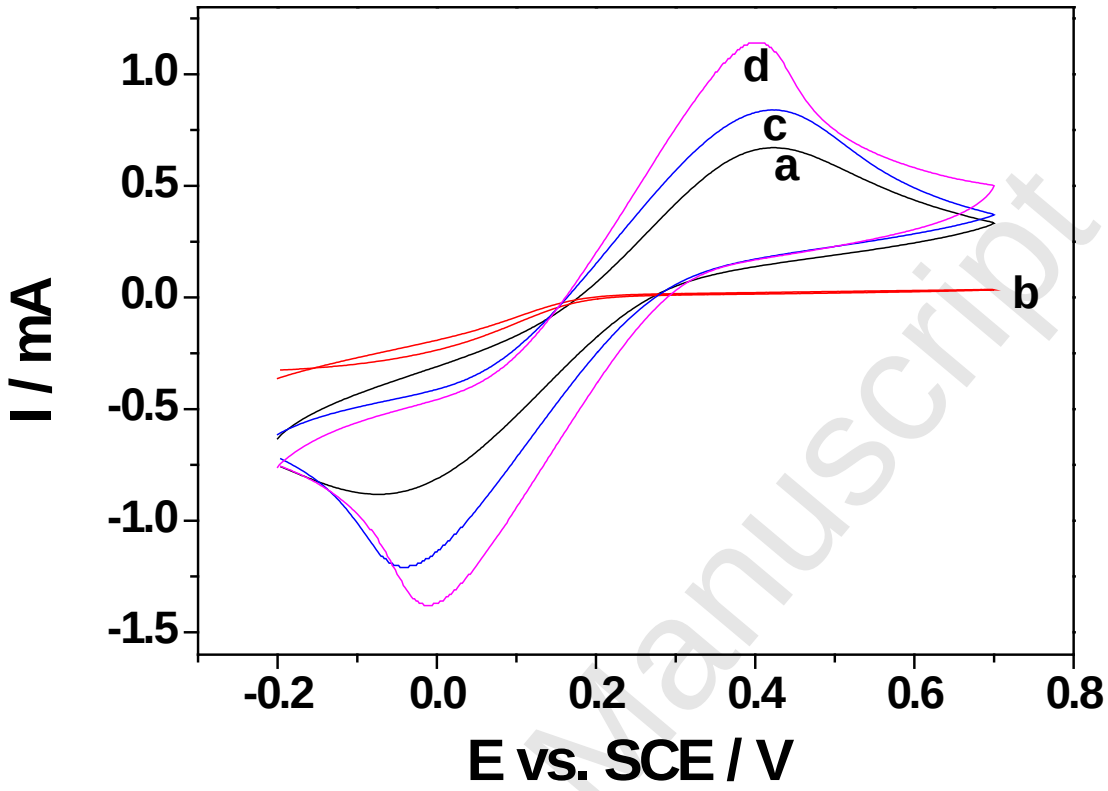

Fig. 5. Cyclic voltammograms of 10 mM $K_3Fe[CN]_6$ in pH 7.0 PB at a bare ITO electrode (a), and ITO electrodes modified with $[PEI/PSS/(PDDA/PSS)_3]$ (b), $[PEI/PSS(PDDA/MWCNT)_3]$ (c), and $[PEI/PSS/(PDDA/MWCNT)_3/Au\ NPs]$ (d). Scan rate = 50 mV/s.

Accepted Manuscript

ACCEPTED MANUSCRIPT

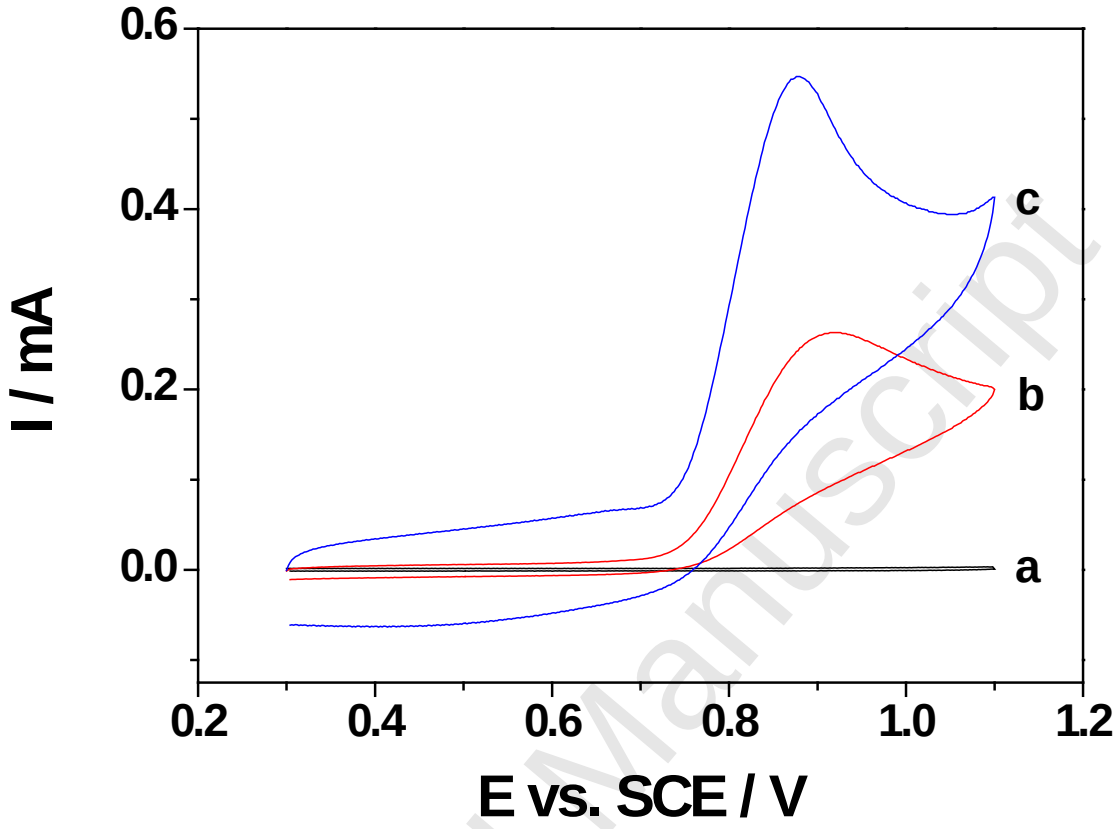

Fig. 6. Cyclic voltammograms obtained in a pH 2.0 0.6 mM $NaNO_2$ solution using a bare ITO electrode (a), and ITO electrodes modified with [PEI/PSS/(PDDA/MWCNT)$_3$] (b) and [PEI/PSS/(PDDA/MWCNT)$_3$/Au NPs] (c). Scan rate = 50 mV/s.

Accepted Manuscript

ACCEPTED MANUSCRIPT

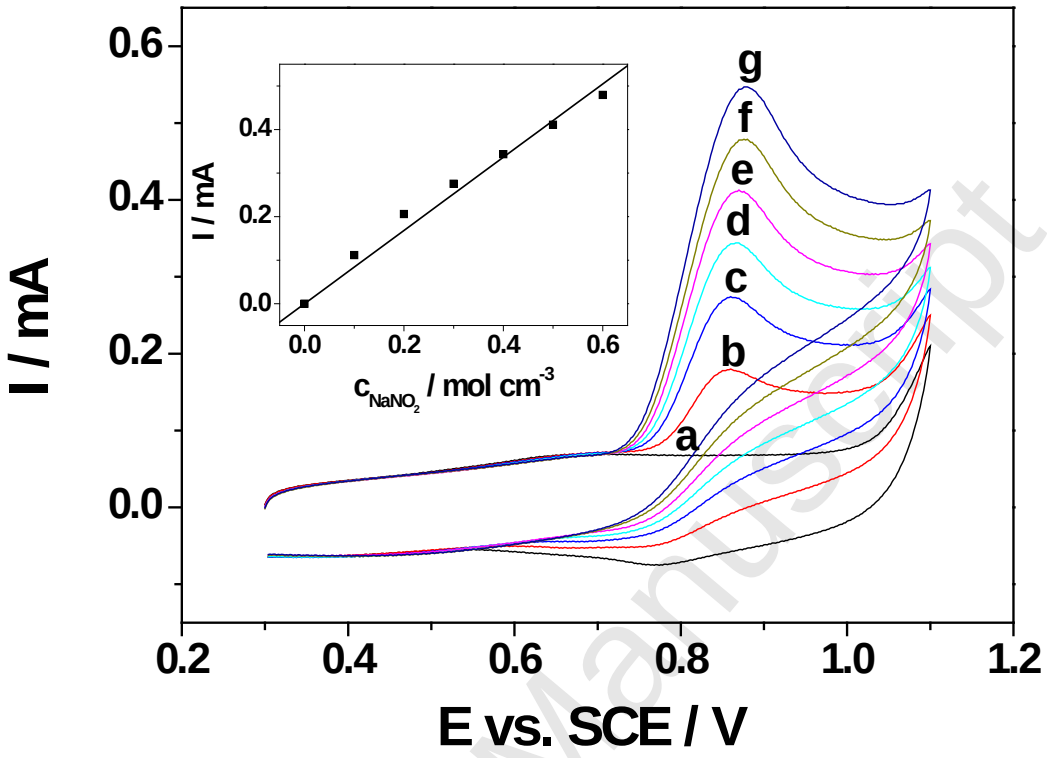

Fig. 7. Cyclic voltammograms of an ITO electrode modified with PEI/PSS/(PDDA/MWCNT)$_3$/Au NPs in pH 2.0 PB buffer containing (a) 0, (b) 0.1, (c) 0.2, (d) 0.3, (e) 0.4, (f) 0.5 (g) 0.6 mM $NaNO_2$. Scan rate = 50 mV/s.

Accepted Manuscript